Talanta 140 (2015) 143–149

Contents lists available at ScienceDirect

Talanta

journal homepage: www.elsevier.com/locate/talanta

Sensitive detection of carcinoembryonic antigen using surface plasmon resonance biosensor with gold nanoparticles signal amplification

Rong Li [a,b], Feng Feng [a,b,*], Ze-Zhong Chen [b], Yun-Feng Bai [b], Fang-Fang Guo [b], Fang-Ying Wu [a], Gao Zhou [a]

[a] Department of Chemistry, Nanchang University, Nanchang 330047, PR China
[b] College of Chemistry and Environmental Engineering, Datong University, Datong 037009, PR China

ARTICLE INFO

Article history:
Received 3 December 2014
Received in revised form
17 March 2015
Accepted 22 March 2015
Available online 30 March 2015

Keywords:
Surface plasmon resonance
Carcinoembryonic antigen
Immunoassay
Gold nanoparticles
Cancer biomarker

ABSTRACT

A new method for real-time detection of carcinoembryonic antigen (CEA) in human serum with high sensitivity and selectivity using surface plasmon resonance (SPR) biosensor was developed. Two kinds of antibodies were used to recognize CEA at different epitopes with high affinity and specificity. Gold nanoparticles (GNPs) modified with streptavidin (SA) were used to further enhance signal specifically via biotin–streptavidin interaction. The binding capacity of the streptavidin-modified gold nanoparticles (SA–GNPs) for ligand biotin was quantified by titration with biotin (5-fluorescein) conjugate to be 10.54 biotin binding sites per 100 nm^2. The developed GNPs enhanced sandwich SPR biosensor successfully fulfilled the sensitive detection of CEA in the range of 1–60 ng/mL with a detection limit of 1.0 ng/mL. Compared to the direct assay format, sandwich format without GNPs and SA–GNPs enhanced sandwich format led to 4.2-fold and 13.8-fold in the sensitivity, respectively. This sensor also showed good selectivity for CEA in the interference study. The results demonstrated that the proposed method could provide a high sensitivity and selectivity in the detection of CEA and offer a promising alternative for cancer biomarker than traditional clinical examinations.

1. Introduction

In recent years, biomarkers, chemical and biological substances that increase in concentration during the formation of cancer, have given important information for early diagnosis, effective treatment and prognosis of cancer [1]. Carcinoembryonic antigen, a cell adhesion glycol–protein that has 70 kD molecular weight normally and becomes 180 kD when glycosylated, is a widely used tumor marker for diagnostic and therapeutic purposes in gastrointestinal, breast and lung cancer [2]. The increase in CEA level in serum above the normal value (2.5 ng/mL, 5 ng/mL for smokers) is an indication of possible disease [3]. Therefore, detection of CEA with high sensitivity and specificity in clinical level is crucial to cancer patients.

Many different analytical methods for determination of CEA such as electrochemical [4–6], fluorometric analysis [7–9], enzyme-linked immunoassay [10] and chemiluminescence immunoassay [11–13] provide sensitive and specific techniques, but generally require multiple steps and time-consuming procedures such as labeling and sample treatment prior to detection. However, these labeling methods are not suitable in some cases, because labeling materials may occupy the important binding sites or cause steric hindrance, resulting in false information. Surface plasmon resonance (SPR), an optical phenomenon occurred in total internal reflection of light at a metal film–liquid interface [14], is one of the powerful analytical techniques for direct monitoring of molecular interactions, without the need for intrinsic or extrinsic labeling to the target molecules. Biosensors based on SPR have been extensively used to monitor molecular interactions for its outstanding sensitivity, reliability, reproducibility as well as its capability to monitor multiple interactions successively [15,16]. SPR biosensors have been applied for the detection of CEA in previous studies [17,18]. SPR based biosensors have also been used for the detection of other biomarkers such as gastric carcinoma-associated antigen MG7-Ag [19], vascular endothelial growth factor receptor (sVEGFR-1) [20] and prostate specific antigen (PSA) [21].

To obtain clinically relevant results, it is essential to improve the sensitivity and enhance the signal. A series of strategies was employed to achieve this goal such as the use of secondary antibodies [17,18,21], functionalized nanoparticles [22–24], quantum dots [25,26] and atom transfer radical polymerization [27]. Due to their huge mass, high dielectric constant, and electromagnetic

* Corresponding author at: Department of Chemistry, Nanchang University, Nanchang 330047, PR China. Tel.: +86 352 7158662; fax: +86 352 6100028.
E-mail address: feng-feng64@263.net (F. Feng).

http://dx.doi.org/10.1016/j.talanta.2015.03.041
0039-9140/

coupling between GNPs and Au film, GNPs have been used widely in a variety of works [21,23,28–33].

In this paper, we developed a novel method to detect CEA in buffer and human serum spiking samples using a SPR biosensor with GNPs to enhance signal. Different methods were used to enhance and amplify the signal including sandwich immunoassay and the second signal amplification by SA–GNPs. The results show that it can be used to detect CEA in buffer or in spiking serum samples with sensitivity and selectivity and realize early diagnosis of cancer in an invasive surgical procedure.

2. Experimental

2.1. Reagents

CEA, alpha fetal protein (AFP), and PSA were obtained from Zhengzhou Biocell antibody center (Zhengzhou, China). Mouse anti-CEA antibodies (clone number: C3) (mAbCEA-C3), mouse anti-CEA antibodies (clone number: B5) (mAbCEA-B5), biotin conjugated mouse anti-CEA antibodies (bio-mAbCEA-B5) and streptavidin were purchased from Bioss (Beijing, China). Bovine serum albumin (BSA) was purchased from Aladdin (Shanghai, China). N-hydroxysuccinimide (NHS), 1-ethyl-3-(3-dimethylaminopropyl)-carbodiimide (EDC), 10 nm gold nanoparticles (5.38×10^{12}–6.5×10^{12} particles/mL) and biotin (5-fluorescein) conjugate were purchased from Sigma-Aldrich. The human serum was from healthy patient in affiliated Hospital of Datong university. All reagents were of analytical grade and used without further purification. Deionized water was used for the preparation of aqueous solution.

2.2. Instrumentations

A two-channel Biacore X™ (Uppsala, Sweden) and CM5 sensor chips were used for the assays. Running buffer was phosphate buffer solution (PBS, 0.01 M phosphate solution, 0.0027 M potassium chloride and 0.137 M sodium chloride, pH 7.4). The operating temperature of the assays was 25 °C and the flow rate of the buffer was 5 μL/min. The SPR response signals were calculated according to the difference subtracted the signal of the control channel (flow cell 1) (Fc1) from that of channel (flow cell 2) (Fc2). So that non-specific binding and buffer induced bulk refractive index changes can be reduced to minimum. All buffers for experiments were filtered (0.22 μm) and degassed before use.

UV–visible spectra were carried out on an UV/VIS spectrophotometer (Lambda 35, PerkinElmer, USA). A fluorescence spectrophotometer (Hitachi, F-2500, Japan) was used to record excitation and emission spectra.

2.3. Modification of GNPs with SA

SA–GNPs conjugate was used for further amplification. SA–GNPs were prepared according to the literature [34] with some modification. Briefly, 1.0 mL colloidal gold solution was initially adjusted to pH 7.4 using K_2CO_3, and then 1.0 mL of SA (20 μg/mL) was added, after incubated for 12 h at 4 °C in a shaker, the mixture was centrifuged (12,000 rpm) at 4 °C for 1 h, then the obtained SA–GNPs conjugates were resuspended into 0.2 mL pH 7.4 PBS containing 1.0% BSA. Conjugates were stable by storing in refrigerator between 2 and 8 °C for several days.

2.4. Immobilization of antibodies

A CM5 dextran chip was first docked into the Biacore instrument and primed with running buffer (PBS, 10 mM, pH 7.4) at a flow rate of 10 μL/min. N-hydroxysuccinimide (NHS) (0.1 M) was mixed 1:1 with 1-Ethyl-3-(3-dimethylaminopropyl)-carbodiimide (EDC) (0.4 M) and injected (70 μL at 10 μL/min) to activate the surface on the Fc2 of the CM5. This was immediately followed by coating antibodies (mAbCEA-C3) (70 μL at 10 μL/min) prepared in 10 mM sodium acetate buffer (pH 4.3). The surface was then deactivated with ethanolamine (1 M, pH 8.5). Each step, including activation, immobilization, and blocking was carried out for 420 s. Fc1 was activated and then deactivated as a reference flow cell channel and used as the background control. The resulting chip was used as a sensing surface for detecting CEA.

2.5. Quantitative detection of SA on the GNPs surface

The coverage factor of SA on GNPs was detected by the fluorescence quenching value of biotin (5-fluorescein) conjugate [35]. 60 μL 1.0 μg/mL biotin (5-fluorescein) conjugate in 10 mM PBS buffer (pH 7.4) and various volumes of 1.0 μg/mL SA in 10 mM PBS buffer were mixed in a centrifuge tube and the total volume was adjusted to 2.0 mL with PBS and incubated for 30 min in the dark. The fluorescence of the solution was measured at $\lambda_{ex}/\lambda_{em}$=492 nm/522 nm with a spectrophotometer, which excitation and emission slits were set at 5 nm and 5 nm, respectively. The changes of fluorescence intensity were plotted as a function of the SA concentrations. The fluorescence of one-tenth volume of total supernatant was determined to quantify the amount of SA in the supernatant.

2.6. Quantitative detection of the binding sites of SA on the GNPs surface

Various volumes of 1.0 μg/mL biotin (5-fluorescein) conjugate in 10 mM PBS buffer and supernatant containing the SA–GNPs were added into a centrifuge tube and the total volume was adjusted to 2.0 mL with PBS and incubated for 30 min in the dark. Control titrations without SA and with solution containing 2.0 μg SA were performed with same procedure. The fluorescence was measured at $\lambda_{ex}/\lambda_{em}$=492 nm/522 nm with slits set at 5 nm and 5 nm. Fluorescence intensity was plotted as a function of the concentrations of free biotin (5-fluorescein) conjugate. The increasing part of this function was linearly fitted and the *x*-axis intercept was used to quantify the binding sites of the immobilized SA on the GNPs surface.

2.7. CEA detection assay

CEA solutions were prepared by diluting into appropriate concentrations (1–700 ng/mL) with PBS. These solutions were then injected over mAbCEA-C3 modified surfaces for 6 min to allow binding assays. Following this, the sensor surface was regenerated by injection of 100 mM HCl (1 min) or the assay was continued to perform a sandwich assay. For the sandwich assay, after the binding of CEA to the sensor surface, 4 μg/mL mAbCEA-B5 was injected on the sensor surface for 6 min. To obtain much more sensitive results, SA–GNPs were used for further amplification. After the binding of CEA to the sensor surface, 4 μg/mL bio-mAbCEA-B5 and then 4.25 μg/mL SA–GNPs were injected to the sensor surface. After a 3 min dissociation period under running buffer flow, the surface was regenerated by injection of 100 mM HCl (1 min) and 20 mM NaOH (0.5 min).

In order to demonstrate whether the binding of CEA to mAbCEA-C3 was solely through the antigen-specific targeting pattern, other cancer biomarkers AFP and PSA were treated with the same strategy to test the cross-reaction. All the data points presented are the averages of triplet measurements unless otherwise stated.

2.8. Detection of CEA in spiking serum sample

Human serum was diluted 1000-fold by PBS buffer containing 0.05% Tween 20 (PBS/T) and then different amount of CEA were spiked into the diluted serum. For SPR assay, the diluted serum were injected to the sensor surface, and then 4 μg/mL bio-mAb-CEA-B5, 4.25 μg/mL SA–GNPs were injected to the sensor surface.

3. Results and discussion

3.1. Detection methodology

Our methodology for the GNPs enhanced SPR detection of CEA with high sensitivity is outlined in Scheme 1. Prior to performing SPR measurements, mAbCEA-C3 was immobilized on CM5 surface via amino coupling. With this method, carboxyl groups of dextran matrix on the sensor ship were first activated with a mixture of EDC and NHS to give reactive succinimide esters (Scheme 1a). The mAbCEA-C3 was then passed over the surface and esters react spontaneously with amino groups to link mAbCEA-C3 covalently to the dextran. After the injection of mAbCEA-C3, ethanolamine was passed over the surface to deactivate the remaining active esters (Scheme 1b). The whole sensorgram is shown in Fig. 1A.

In the presence of CEA, CEA was captured by mAbCEA-C3 with high specificity and affinity (Scheme 1c). After CEA was first captured on a mAbCEA-C3 modified CM5 surface, mAbCEA-B5, interacts with CEA at a different epitope than that of mAbCEA-C3, were injected quickly to the flow cell quickly to fabricate mAbCEA-C3/CEA/bio-mAbCEA-B5 sandwich assay format (Scheme 1d). Then SA–GNPs were injected quickly to the mAbCEA-C3/CEA/bio-mAbCEA-B5 complex to further amplify the signal to fabricate GNPs enhanced sandwich assay format (Scheme 1e). The corresponding processes were shown with the sensorgram in Fig. 1B.

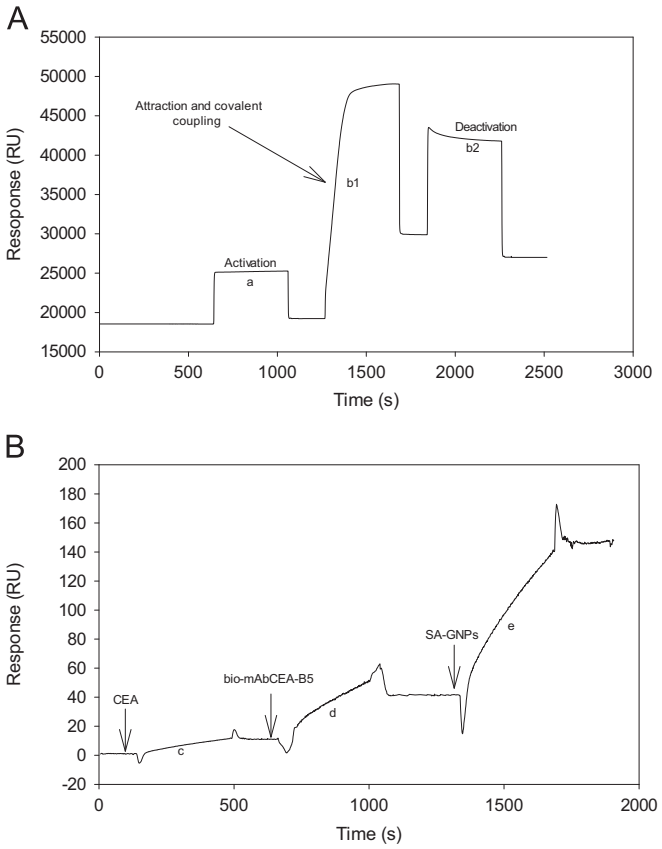

Fig. 1. (A) Sensorgrams of process of immobilization of mAbCEA-C3. (B) Senso rgrams of process of CEA detection using GNPs enhanced sandwich assay (CEA was 10 ng/mL).

3.2. Detection of CEA in direct format

A standard direct binding assay was carried out on the prepared surface. The SPR response–time curves were used to monitor the reaction progress between mAbCEA-C3 and CEA. The typical sensorgram was shown in Fig. 2A, which indicated that the response increased with the increment of CEA concentration. When the running solution was switched from PBS buffer to CEA, the response change increased due to the binding of CEA to mAbCEA-C3 that immobilized on the sensor surface. The calibration plot displayed a good linear relationship between SPR response and CEA concentration in the range of 50–500 ng/mL with a correlation coefficient of 0.9977 (Fig. 2B). The limit of detection (LOD) was calculated as the signal obtained from the CEA concentration that was equivalent to 3 times the standard deviation of the signals obtained from the blank standards. The LOD of direct detection of CEA was 13.78 ng/mL. Normal value of CEA in human serum ranges between 2.5 and 5 ng/mL. Therefore, it is important to develop the method with detection limit 2.5 ng/mL or lower to cover this fact. It was not sufficient for detection of normal levels in direct format. So it is crucial to improve the detection sensitivity.

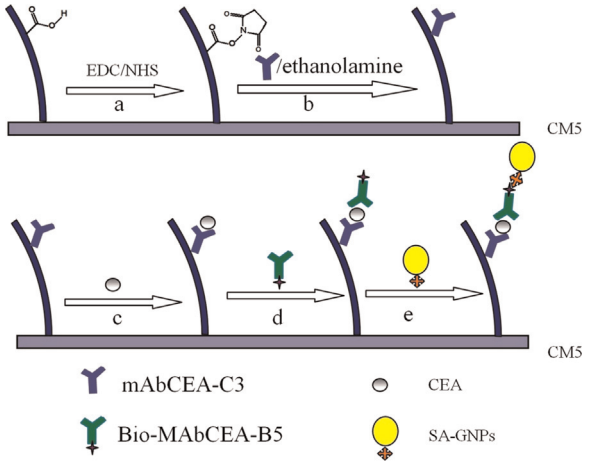

Scheme1. The methodology of CEA detection using SA–GNPs enhanced sandwich format.

3.3. mAbCEA-B5 enhanced sandwich format for CEA detection

As an alternative to improve the detection sensitivity of CEA, a sandwich assay was used to detect CEA antigen at very low concentrations. In this work, mAbCEA-C3 was selected as the anchor antibody to be immobilized onto the sensor surface, and mAbCEA-B5 as the second antibody for the sandwich assay. Fig. 3A illustrated mAbCEA-B5 enhanced response signal as a function of CEA concentration. A linear dependence of the SPR response on the CEA concentrations was observed at lower concentrations in the range of 5–80 ng/mL with a correlation coefficient of 0.9973 (Fig. 3B). The LOD of this enhanced sandwich assay for CEA detection was reduced to 3.30 ng/mL. The method of the sandwich assay with mAbCEA-B5 gave about 4.2-fold enhancement in the sensitivity compared to that of the direct detection method. Therefore, it can be concluded that the two kinds of antibodies are able to bind to different epitopes of CEA antigen, and the sandwich

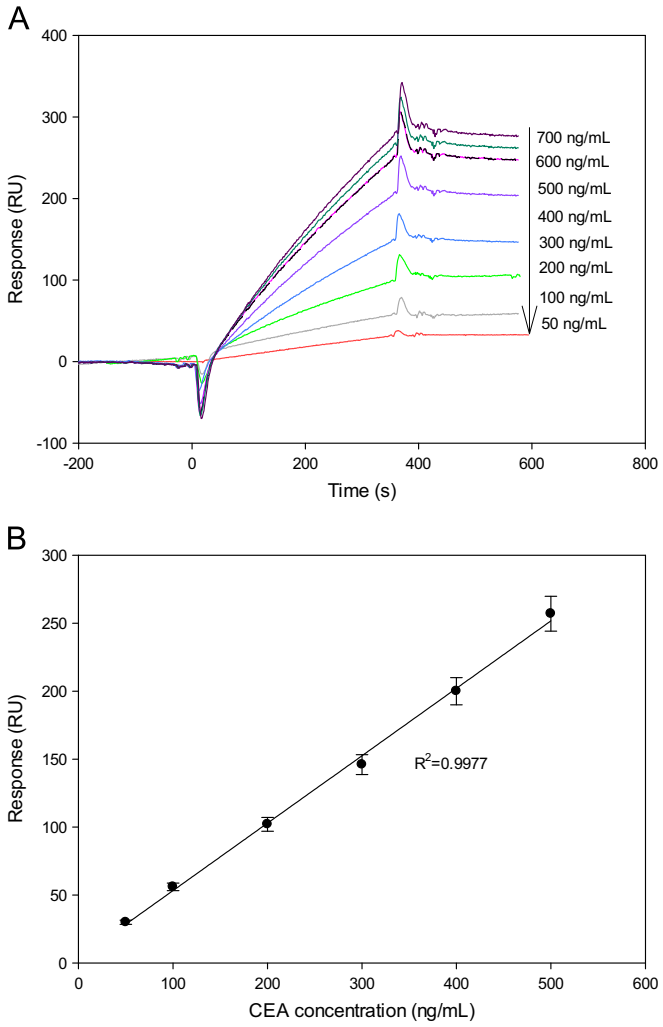

Fig. 2. (A) Response of different concentrations of CEA in direct format (50, 100, 200, 300, 400, 500, 600, and 700 ng/mL from bottom to top). (B) Calibration curve of CEA response. Error bars represent the standard deviations for three replicates.

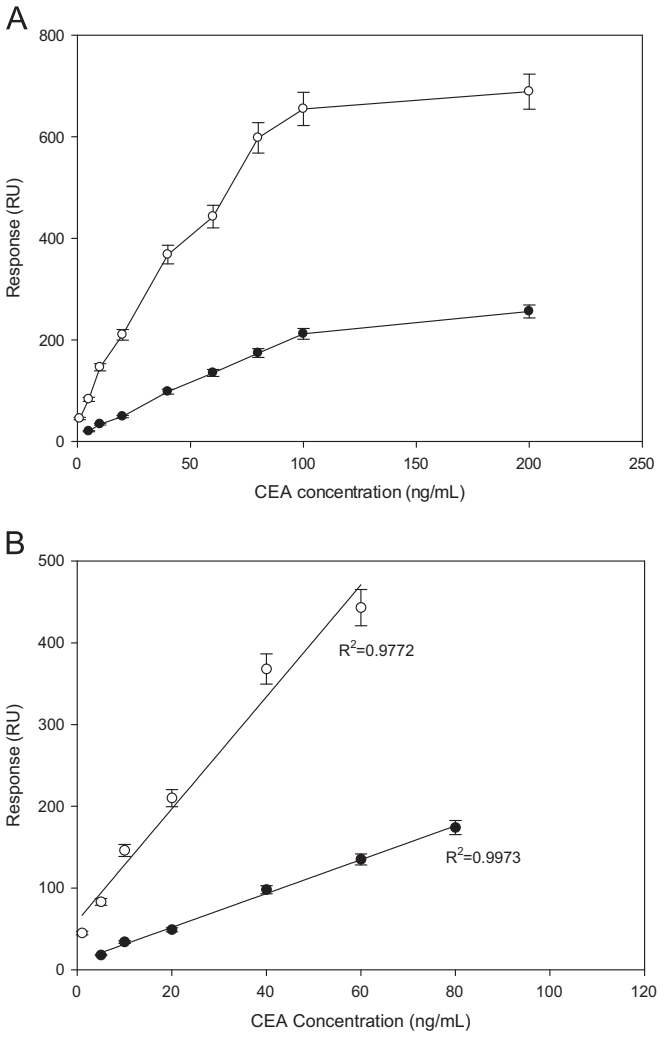

Fig. 3. (A) Response curve of CEA in sandwich detection format (•) and SA–GNPs enhanced sandwich detection format (○) and (B) calibration curve of CEA in sandwich detection format (•) and SA–GNPs enhanced sandwich detection format (○). Error bars represent the standard deviations for three replicates.

assay amplifies the original interaction signal significantly but it was not still low enough to detection of normal levels of CEA.

3.4. SA–GNPs enhanced sandwich format for CEA detection

To further amplification, GNPs enhanced sandwich assay using bio-mAbCEA-B5 and SA–GNPs were conducted because GNPs can cause high resonance angle shift due to their participation in surface plasmon resonance and hence increase the signal obtained from the sensor [36].

The sandwich assay with GNPs enabled the detection of CEA levels as low as 1.0 ng/mL. Fig. 3A illustrated SA–GNPs enhanced response signal as a function of CEA concentration. As expected, the observed response signal was increased as the CEA concentration increased. The calibration plot showed a good linear relationship between SPR response and CEA concentration in the range of 1–60 ng/mL with a correlation coefficient of 0.9772 (Fig. 3B). The LOD of this enhanced sandwich assay for CEA in detection by SPR biosensor was 1.0 ng/mL, which was being below required value of 2.5 ng/mL.

Comparing the three calibration curves (Figs. 2B and 3B), the sensitivity of GNPs enhanced sandwich assay format was about 13.8-fold better than that using direct assay format and 3.3-fold better than that using sandwich assay format without GNPs. Obviously, the detection of the low CEA concentration benefits from the introduction of the gold enhancement steps.

To confirm that the gold labeling interaction was specifically mediated through the biotin–streptavidin interaction, bio-mAb-CEA-B5 was substituted by mAbCEA-B5. The results showed that no significant enhancement was observed using mAbCEA-B5 but the significant enhancement was obtained using the biotinylated mAbCEA-B5 (Fig. 4). It is indicated that the labeling interaction was specifically via recognition of SA to biotin not nonspecific adsorption.

3.5. Characterization of SA–GNPs

The bioconjugation of SA–GNPs was confirmed by UV–vis absorption spectra (Fig. 5). The SA solution and GNPs showed an absorption peak at nearly 280 nm and 520 nm, respectively. The GNPs solution was redshifted 10 nm after conjugated with SA, indicating that SA was successfully attached to the GNPs surface.

3.6. Quantitative detection of SA adsorbed to the GNPs surface using biotin (5-fluorescein) conjugate

To quantify evaluate the amount of SA adsorbed to the GNPs, fluorescence titration experiments were performed using a

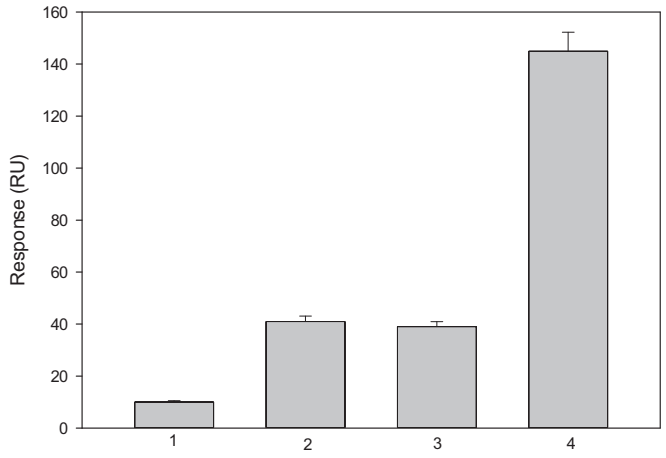

Fig. 4. SPR signal for (1) mAbCEA-C3/CEA, (2) mAbCEA-C3/CEA/mAbCEA-B5, (3) mAbCEA-C3/CEA/mAbCEA-B5/SA–GNPs, and (4) mAbCEA-C3/CEA/bio-mAbCEA-B5/SA–GNPs. The concentration of CEA, mAbCEA-B5, bio-mAbCEA-B5 and SA–GNPs were 10 ng/mL, 4 μg/mL, 4 μg/mL, and 4.25 μg/mL respectively. Error bars represent the standard deviations for three replicates.

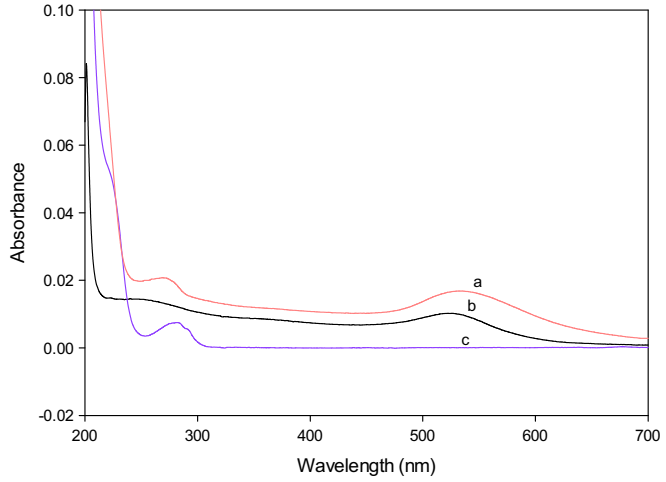

Fig. 5. UV–vis absorption spectra of (a) SA–GNPs, (b) GNPs, and (c) SA.

fluorescently labeled SA ligand, biotin(5-fluorescein) conjugate, to evaluate the amount of SA adsorbed to the GNPs. When SA interacts with biotin-(5-fluorescein) conjugate by molecular recognition of its binding site, its fluorescent activity is effectively quenched. The decrease value of fluorescence intensity is proportional to the amount of the added SA. Liquid handling and a fluorometer are needed to quantification of SA binding properties. Standard curve was obtained by the following steps: various volumes SA of a certain concentration were added into tubes containing a fixed quantity of biotin (5-fluorescein) conjugate and then adjusted to the total volume 2.0 mL. The fluorescence of the solution was measured after incubating and the fluorescence intensity are plotted as a function of the mass of added SA (Fig. 6). This line is used as reference line for quantification of the amount of SA in supernatant after removal of the GNPs. 200 μL of total supernatant in buffer was measured the fluorescence intensity with the same procedure. The amount of SA adsorbed to GNPs was calculated to be 8.50 μg according to the difference subtracted the amount in supernatant from the total amount added. The results show that 42.5% of SA adsorbed to the GNPs and 57.5% of SA remains in the supernatant.

3.7. *Quantitative detection of the binding sites of SA adsorbed to the GNPs surface using biotin (5-fluorescein) conjugate*

To evaluate the accessibility of the binding sites of immobilized SA, fluorescence titration experiments were also implemented using biotin (5-fluorescein) to quantify the number of binding sites. The approachability of the binding sites of the SA–GNPs conjugate was measured by following steps: various volumes of a certain concentration of biotin (5-fluorescein) conjugate were added into each tube containing a fixed amount of SA and then the total volume was adjusted to 2.0 mL. The fluorescence of the solution was measured after incubating. Fig. 7 illustrated fluorescence intensities changes as a function of the mass of the added biotin (5-fluorescein) conjugate. In the absence of SA, the calibration plot showed a good linear relationship between fluorescence intensity and biotin concentration with a correlation coefficient of 0.9960. This line was used as reference line for all further experiments. In contrast, a titration was performed in the presence of simple or nanoparticle-conjugated SA, no fluorescence was observed until all biotin binding sites were occupied. When binding sites of SA were fully occupied, a parallel

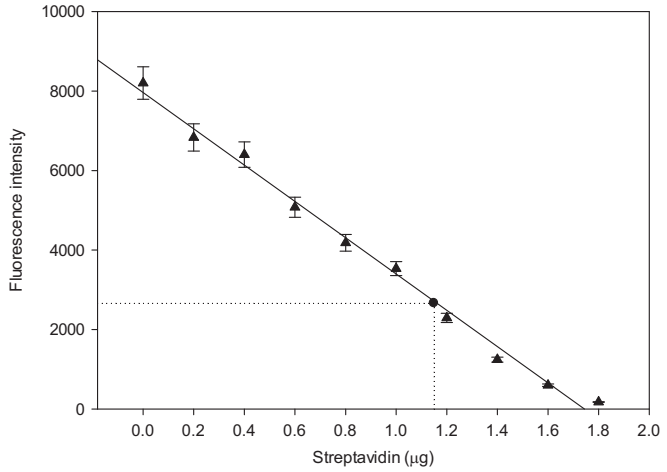

Fig. 6. Changes of fluorescence intensity with the amount of SA added to 60 μl, 1.0 μg/mL biotin (5-fluorescein) conjugate solution in 10 mM PBS buffer. The dotted line represents SA in the supernatant. Error bars represent the standard deviations for three replicates.

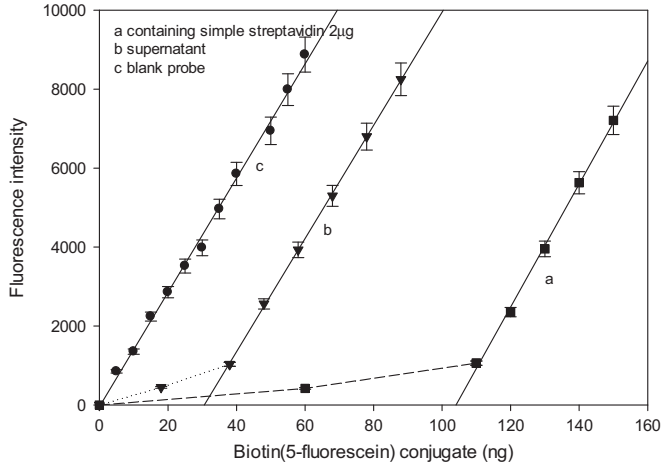

Fig. 7. Fluorescence intensity functions by titration of biotin (5-fluorescein) to a set of samples used to determine of the biotin-binding capacity of GNPs functionalized with SA. The set of samples consisted of three different solutions: (a) a buffer containing simple SA (2 μg), (b) the supernatant of the SA–GNPs suspension after removal of GNPs, and (c) a blank probe containing only PBS buffer. Error bars represent the standard deviations for three replicates.

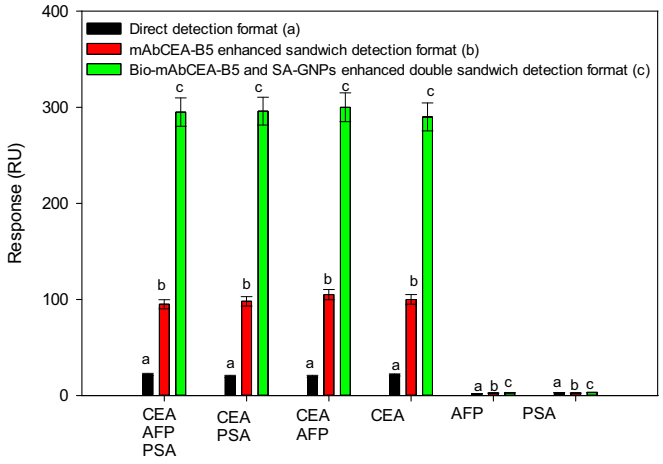

Fig. 8. Detection of mixture of CEA, PSA and AFP using different format. Black columns (a) indicate the signal in direct detection format. Red columns (b) indicate the signal in mAbCEA-B5 enhanced sandwich detection format. Green columns (c) indicate the signal in SA–GNPs enhanced sandwich detection format. Concentrations of CEA, PSA, and AFP were 40 ng/mL, 1 μg/mL, and 1 μg/mL, respectively. (For interpretation of the references to color in this figure legend, the reader is referred to the web version of this article.)

Table 1
Detection of CEA in diluted human serum samples.

No.	CEA added (ng/mL)	CEA tested[a] (ng/mL)	Recovery (%)	RSD (%)
1	10	11.01	110.10	5.03
2	20	20.32	101.60	10.87
3	50	51.85	103.70	4.96
4	80	82.05	102.56	7.63
5	100	106.86	106.86	8.99

[a] Mean values of three determinations.

line to the reference line was observed but shifted by a certain off-set. This off-set of simple SA set to 100% of accessible SA binding sites. From the off-set of the line, the number of accessible biotin binding sites in the SA solution or suspension was calculated. The accessibility of the binding sites of the immobilized SA was quantified from the data displayed in Fig. 7 This value corresponding directly to the accessibility of the binding sites of the particle-conjugated SA was 5.90 μg and resulted in values of 69.4% SA immobilized on the GNPs surface.

The average diameter of GNPs was 10 nm, a functional surface group density of 3.80 SA molecules 100 nm^{-2} are introduced by electrostatic adsorption or, in other terms, about 11.92 SA tetramer molecules are bound to one particle and about 33.10 biotin binding sites are accessible at the surface of a single particle. This corresponds to 10.54 biotin binding sites per 100 nm^2 particle surface.

3.8. Selectivity of the strategy

Selectivity is another critical factor to assess the performance of the proposed sensor. To test the selectivity of the present SPR immunosensor, control experiments were performed using substituting CEA by AFP or PSA. As shown in Fig. 8, with the non-target protein, no signal change was observed compared with CEA. In addition, the mixture samples, prepared by mixing 40 ng/mL CEA, 1.0 μg/mL AFP and 1.0 μg/mL PSA, were also measured on this platform. As shown in Fig. 8, when the concentration of CEA is 0 ng/mL, the SPR responses of immunosensor is very low, indicating a relatively low background response. The SPR responses of immunosensor with interferential species at high concentration of 1.0 μg/mL are just a little higher than that of the immunosensor with 40 ng/mL CEA. These results demonstrated that the proposed sandwich SPR biosensor can effectively distinguish CEA from other proteins.

3.9. Application of the SPR biosensor for the detection of CEA in biological samples

To investigate the reliability of this constructed SPR biosensor for real samples, several samples were prepared by spiking different amounts of CEA into human serum samples that has been diluted 1000-fold by PBS/T buffer to minimize nonspecific adsorption. The results are summarized in Table 1. The recovery (between 101.60% and 110.10%) and relative standard deviation (RSD) (between 4.96% and 10.87%) were acceptable, which indicated that the developed SPR biosensor provides a possible application for the detection of CEA in clinical diagnostics.

4. Conclusions

In this work, a novel method of sensitive detection of CEA based on SPR biosensor using SA–GNPs to amplified signal has been developed. The binding capacity of SA–GNPs for ligand biotin was determined by quenching of the fluorescence upon binding due to molecular recognition. Different detection formats including direct detection format, sandwich detection format and GNPs enhanced sandwich detection format were used to detect CEA in buffer and spiking human serum samples. Using bio-mAbCEA-B5 and SA–GNPs enhanced sandwich detection format, a minimum LOD of 1.0 ng/mL was obtained. The assay enables the detection of CEA levels at clinical relevant concentration. This sensor also showed good selectivity for CEA without interference of some other cancer biomarker, such as AFP and PSA. The experimental results confirmed that the proposed SPR biosensor possessed high sensitivity and good selectivity for CEA detection. It is a promising method for sensitive, selective and reliable diagnosis for gastrointestinal, breast and lung cancer.

Acknowledgments

We acknowledge the financial support from the National Natural Science Foundation of China (21175085 and 21375083).

References

[1] M. Perfézou, A. Turner, A. Merkoci, Chem. Soc. Rev. 41 (2012) 2606–2622.
[2] A. Aquino, V. Formica, S.P. Prete, P.P. Correale, M.C. Massara, M. Turriziani, L.D. Vecchis, E. Bonmassar, Pharm. Res. 49 (2004) 383–396.
[3] F.G. Fernandez, J.A. Drebin, D.C. Linehan, F. Dehdashti, B.A. Siegel, S.M. Strasberg, Ann. Surg. 240 (2004) 438–447.
[4] Z.Y. Zhong, W. Wu, D. Wang, D. Wang, J.L. Shan, Y. Qing, Z.N. Zhang, Biosens. Bioelectron. 25 (2010) 2379–2383.
[5] J.Y. Liu, J. Wang, T.S. Wang, D. Li, F.N. Xia, J. Wang, E.K. Wang, Biosens. Bioelectron. 65 (2015) 281–286.
[6] Z. Altintas, S.S. Kallempudi, U. Sezerman, Y. Gurbuz, Sens. Actuators B 174 (2012) 187–194.
[7] J.Y. Hou, T.C. Liu, G.F. Lin, Z.X. Li, L.P. Zou, M. Li, Y.S. Wu, Anal. Chim. Acta 734 (2012) 93–98.
[8] J.W. Ma, Q.S. Fan, L.H. Wang, N.Q. Jia, Z.D. Gu, H.B. Shen, Talanta 81 (2010) 1162–1169.
[9] K.Q. Wu, C.C. Chu, C. Ma, H.M. Yang, M. Yan, S.G. Ge, J.H. Yu, X.R. Song, Sens. Actuators B 206 (2015) 43–49.
[10] F. Zhou, M.M. Wang, L. Yuan, Z.P. Cheng, Z.Q. Wu, H. Chen, Analyst 137 (2012) 1779–1784.
[11] L.L. Chen, Z.J. Zhang, P. Zhang, X.M. Zhang, A.H. Fu, Sens. Actuators B Chem. 155 (2011) 557–561.
[12] X.H. Fu, R. Huang, J.Y. Wang, B. Chang, RSC Adv. 3 (2013) 13451–13456.
[13] C. Wang, J. Wu, C. Zong, H.X. Ju, F. Yan, Analyst 136 (2011) 4295–4300.

[14] M. Piliarik, H. Vaisocherová, J. Homola, J. Methods Mol. Biol. 503 (2009) 65–68.
[15] R.L. Rich, D.G. Myszka, Curr. Opin. Biotechnol. 21 (2000) 54–64.
[16] L. Huang, G. Reekmansa, J.M. Friedta, F. Frederixa, L. Francisa, S. Muyldermansb, A. Campitellid, C.V. Hoof, Biosens. Bioelectron. 21 (2005) 483–490.
[17] Z. Altintas, Y. Uludag, Y. Gurbuz, I.E. Tothilla, Talanta 86 (2011) 377–383.
[18] F.Y. Su, C.Y. Xu, M. Taya, K. Murayama, Y. Shinohara, S.I. Nishimura, Sensors 8 (2008) 4282–4295.
[19] X.Y. Fang, Y.H. Xie, Q.J. Li, Q.C. Zhao, D.M. Fan, Cancer Epidemiol. 34 (2010) 648–651.
[20] K. Pimková, M. Bocková, K. Hegnerová, J. Suttnar, Anal. Bioanal. Chem. 402 (2012) 381–387.
[21] Y. Uludag, I.E. Tothill, Anal. Chem. 84 (2012) 5898–5904.
[22] J.L. Wang, Z.Z. Zhu, A. Munir, H.S. Zhou, Talanta 84 (2011) 783–788.
[23] M.J. Kwon, J. Lee, A.W. wark, H.J. Lee, Anal. Chem. 84 (2012) 1702–1707.
[24] Y. Wang, J. Dostalek, W. Knoll, Anal. Chem. 83 (2011) 6202–6207.
[25] A. Shabani, M. Tabrizian, Analyst 138 (2013) 6052–6062.
[26] G.P. Anderson, R.H. Glaven, W.R. Algar, K. Susumu, M.H. Stewart, I.L. Medintz, E.R. Goldman, Anal. Chim. Acta 786 (2013) 132–138.
[27] Y. Liu, Q. Cheng, Anal. Chem. 84 (2012) 3179–3186.
[28] J.S. Mitchell, Y.Q. Wu, C.J. Cook, L. Main, Anal. Biochem. 343 (2005) 125–135.
[29] J.S. Mitchell, T.E. Lowe, Biosens. Bioelectron. 24 (2009) 2177–2183.
[30] W.C. Law, K.T. Yong, A. Baev, P.N. Prasad, ACS Nano 5 (2011) 4858–4864.
[31] J. Martinez-Perdiguero, A. Retolaza, L. Bujanda, S. Merino, Talanta 119 (2014) 492–497.
[32] L. He, M.D. Musick, S.R. Nicewarner, F.G. Salinas, S.J. Benkovic, M.J. Natan, C.D. Keating, J. Am. Chem. Soc. 122 (2000) 9071–9077.
[33] Y.F. Bai, F. Feng, L. Zhao, C.Y. Wang, H.Y. Wang, M.Z. Tian, J. Qin, Yl Duan, X.X. He, Biosens. Bioelectron. 47 (2013) 265–270.
[34] L.A. Lyon, M.D. Musick, M.J. Natan, Anal. Chem. 70 (1998) 5177–5183.
[35] T. Schiestel, H. Brunner, G.E.M. Tovar, J. Nanosci. Nanotechnol. 4 (2004) 504–511.
[36] L.A. Lyon, M.D. Musick, P.C. Smith, B.D. Reiss, D.J. Peña, M.J. Natan, Sens. Actuators B 54 (1999) 118–124.